Simulation of combustion in a porous medium with high pressure and temperature conditions

Arash Mohammadi[*,§], Ali Jazayeri[**] Masoud Ziabasharhagh[***]
[*] PhD , K.N.Toosi University of Technology
[**] Associated Professor , K.N.Toosi University of Technology
[***] Associated Professor , K.N.Toosi University of Technology
([§]amohammadi@dena.kntu.ac.ir)

ABSTRACT: Porous media has benefits to enhance evaporation of droplets in liquid-fuel burners, reduce emission of pollutants and minimize instabilities. This paper represents the numerical study of liquid-fuel injection and combustion inside constant-volume chemically inert PM to stabilize lean mixture. 3D numerical results were obtained based on a modified KIVA-3V code. Diesel is directly sprayed inside hot and high pressure PM chamber. Complete evaporation and self-ignited was achieved due to high temperature. The results for an especial condition have compared with an experimental data in literature. Contours of diesel vapor, fluid and solid temperature of PM in azimuthally cross section, were shown. Also, effects of mass of sprayed fuel were studied. The results show considerable reduction in carbon monoxide, nitrogen monoxide and soot formation.

Keywords: Numerical study, Porous medium, diesel conditions

INTRODUCTION

The most important issue of direct-injection IC engines that currently exists is stratified mixture formation in the combustion chamber, which causes heterogeneous heat release, high local in-cylinder temperature and high temperature-gradient in combustion chamber. Therefore, emissions such as NO_x, HC, CO and soot produce. In current strategy, the exhaust emissions of IC engines can be reduced by catalyst converter, but they have high cost and low efficiency. Decrease in emission of IC engines may be achieved with homogeneous mixture formation and a 3D-ignition of homogeneous charge and ensuring homogeneous temperature field. Conventional direct injection engines indicate lack of mechanisms for fuel-air homogenization. PM as an option can be used to achieve this goal [1, 2]. This technique has been used for both gaseous and liquid fuels in steady or unsteady combustion. In the literature there are many researches on gaseous combustion in PM but a few studies investigate liquid-fuel combustion in PM and its capability for mixture formation and combustion processes [3-6]. Considerable features of PM for application to combustion technology are: large specific surface area, excellent heat transfer properties, heat capacity, transparency for fluid flow, thermal resistance mechanical resistance and electrical properties [1, 2].

PM engine is defined as an engine with homogeneous combustion process realized in a PM volume. The following individual processes of PM engine are realized in PM volume: energy recirculation in cycle, fuel injection in PM, fuel vaporization (for liquid fuels), mixing with air, homogenization of charge, 3D-thermal self-ignition, and a homogeneous combustion.

Permanent contact between working fuel and PM-volume in a diesel engine. It is assumed that the PM-combustion chamber is mounted in the engine head. Also, all necessary conditions for homogeneous combustion are carried out in the PM combustion chamber [7].

The first idea to use PM in the IC engines was proposed by Weclas et al. [7, 8]. They investigated the performance of a PM single-cylinder, air-cooled diesel engine, without using of catalyst. They mounted a Silicon Carbide (SiC) PM in the cylinder head. Their results showed increasing in engine efficiency, reducing the emissions and noise in comparison with the original engine. Lee et al. [9] mounted a PM on the piston bowl of single-cylinder diesel engine, and observed increasing in power and reduction in noise relative to original engine. Also, NO_x decreased significantly while, HC and soot increased. Weclas [10, 11] carried out diesel jet impingement on PM with high porosity. Weclas et al. [12-14] investigated penetration of liquid-fuel spray in a PM (as arrangement of cylinders) with different diameters that were mounted on a flat plate, they changed the arrangement of cylinders to find optimum geometry for a PM that could produce the best mixture formation. Weclas et al. [15] studied effect of liquid-fuel injection in an annulus PM. They measured jet penetration of liquid fuel after exit from PM space.

In this study, 3D-CFD simulation of constant free-volume and PM reactor were done with modified version of KIVA-3V code. Diesel was sprayed directly in hot cylindrical PM. Combustion was started with due to heat supply from solid phase of PM. It is demonstrated that complete evaporation and flame stability occurs due to presence of PM. Numerical computations have been compared with experimental data of Weclas et al. [15]. The effects of mass of injected diesel- fuel, on mixture formation and combustion processes, were studied. Mean in-cylinder pressure and temperature of solid phase and gas phase in PM, and mass fraction of $C_{10}H_{22}$, CO, NO versus time, was considered. The results showed capability of PM in control of mixture formation and combustion processes.

GOVERNING EQUATIONS

For simulation of PM engine, some assumptions were used for modeling of the PM, include:

(1) There is thermal non-equilibrium between gas and solid phases.

(2) Solid is homogeneous, isotropic, variable property with temperature and has no catalyst effects.

(3) Radiation heat transfer from the solid phase is considered only and the gas phase is transparent.

Regard to the above assumptions, governing equations are [16, 17, 18]:

Continuity equation:

$$\frac{\partial(\rho_i \varphi)}{\partial t} + \nabla.(\rho_i\, u\, \varphi) = \nabla.\left[\rho\, \varphi\, D_{im} \nabla\left(\frac{\rho_i}{\rho}\right)\right] + \varphi\, \dot{\rho}_i^c + \dot{\rho}^s\ \delta_{i1} \tag{1}$$

φ is porosity of porous media, ρ_i is density of species i and u is velocity vector.

Gas phase momentum equation:

$$\frac{\partial(\rho\, u)}{\partial t} + \nabla.(\rho\, u\, u) = -\frac{1}{a^2}\nabla P - \nabla\left(\frac{2}{3}\,\rho\, k\right) + \nabla.\sigma + F^s - \left(\frac{\Delta P}{\Delta L}\right) \tag{2}$$

$$\left(\frac{\Delta P}{\Delta L}\right) = \left(\frac{\mu}{\alpha}\,\vec{V} + c_2\,\frac{1}{2}\,\rho_g\,|\vec{V}|\,\vec{V}\right) \tag{3}$$

The last term on the right-hand side of Eq. (2) is due to pressure drop caused by PM that Ergan equation was used and σ is stress tensor.

Gas phase energy equation:

$$\frac{\partial}{\partial t}(\varphi\rho c_p T_g) + \nabla.(\varphi\rho c_p T_g u) + \varphi \sum_i \dot{\omega}_i\, h_i W_i = -\varphi P\, \nabla.u + \rho\epsilon + \varphi\, \nabla.\left((k_g + \rho_g c_g D_{\parallel}^d)\nabla T_g\right) - h_v(T_g - T_s) + \dot{Q}^s \tag{4}$$

$$h_v = \frac{6\varepsilon}{d^2} k_g Nu_v \text{ , } Nuv = 2 + 1.1\, Re^{0.6}\, Pr^{0.33} \quad (5)$$

c_p is specific heat of mixture, T_g is gas temperature, Y_i is mass fraction species i, $\dot{\omega}_i$ is rate of reaction i, h_i is enthalpy of species i, W_i is molecular weight of species i, k_g is thermal conductivity of the fluid, $D_{\|}^{d}$ is thermal dispersion coefficient along the length of the porous medium, h_v is volumetric heat transfer coefficient. Correlation (5) was estimated from experimental data by Wakao and Kaguei for heat transfer between packed beds and fluid [17].

Solid phase energy equation:

$$\frac{\partial}{\partial t}\left((1-\varepsilon)\, \rho_s\, c_s\, T_s\right) = \nabla \cdot [k_s\, (1-\varepsilon)\nabla T_s] + h_v \left(T_g - T_s\right) - \nabla . q_r \quad (6)$$

T_s is solid temperature, ρ_s is solid density, c_s is specific heat of solid medium, k_s is thermal conductivity of solid, q_r is the radiation heat transfer in solid.

Chemical species continuity equation:

$$\frac{\partial}{\partial t}\left(\varepsilon\, \rho_g Y_i\right) + \nabla . \left(\varepsilon\, \rho_g Y_i\, \vec{V}\right) + \nabla . \left(\varepsilon\, \rho_g Y_i\, V_i\right) - \varepsilon\, \dot{\omega}_i\, W_i = 0 \quad (7)$$

$$V_i = -\left(D + D_{\|m}^{d}\right) \frac{1}{X_i}\, \nabla X_i \quad (8)$$

X_i is molar fraction of species i, Pe is Peclet number, D_{im} is diffusion coefficient of species i is mixture.

Equation of state:

$$P = \rho_g\, R\, T_g \,/\, \overline{W} \quad (9)$$

R is universal constant of gases, $\overline{W}$ is average molecular weight of mixture, P is pressure inside the combustion chamber and the porous medium.

Combustion model:

Combustion process includes ten equations and twelve species, which includes one-step reaction for methane fuel and Zeldovich mechanism for NO formation. Rate of reactions are computed with Arrhenius method. However, for six other equations that reaction rate is very quick relative to last four equations hence, equilibrium reactions are considered. In order to consider effects of turbulence on combustion, Eddy-Dissipation model [17, 18] has been used.

Radiation model:

Gas phase radiation in comparison with solid phase, that has a high absorption coefficient, is regardless. The heat source term $\nabla . q_r$, due to radiation in solid phase that appears in Eq .12, is calculated from Rosseland [17] method.

$$q_r = -\frac{16}{3} \frac{\sigma\, {T_s}^3}{\beta}\, \nabla T_s \quad (12)$$

σ Boltzmann constant and β is extinction coefficient.

Liquid Spray:

Solving for the essential dynamics of a spray and its interactions with a gas is an extremely complicated problem. In many sprays, drop Weber numbers is larger than unity, and drop oscillations, distortions, and breakup must be considered. Drop collisions and coalescence have also been found to be important in many engine sprays [18].

MESH PREPARATION

Fig. 1 presents schematic geometry of constant-volume PM. Prior to CFD simulation, computational mesh of chamber was generated with Kiva-Prep. The geometry of a mesh is composed of one block. Fig.1 shows the grid configuration of the volume (sector mesh). Mesh size is about 77842 for this computational study. Fig. 2 shows the schematic grid configuration of chamber.

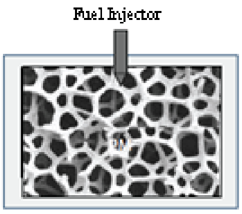

Figure 1. schematic presentation of constant volume PM [16]

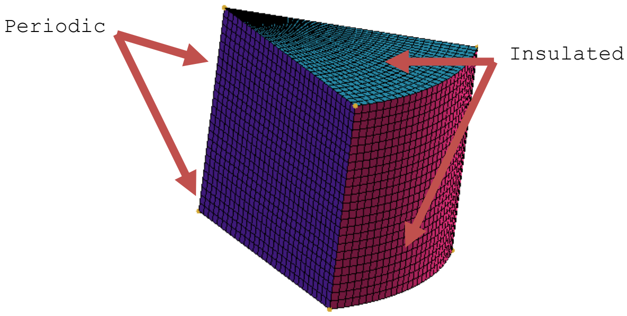

Figure 2. Computational mesh for the PM chamber

INITIAL AND BOUNDARY CONDITIONS

Initial temperature and pressure for fluid flow and PM was assumed 800K, 1000 K and 10, 11 bar respectively. Mass of injected fuel was 1.4 and 3.4 mg with injection duration of 2 ms. Porosity is 90 percent with different pore density range (8-10-20-30 ppi). Initial velocity was assumed 0.0. The entire boundary wall was assumed as insulated (zero heat-flux condition) for fluid and solid phases, in free-volume chamber and SiC PM reactor.

VALIDATION

For validation of numerical simulation, experimental data of Weclas et al. was used. Initial pressure and temperature of both phase are 16 bar and 800 K, respectively. Mass of injected fuel for injector was 3.4 mg. In Fig. 3, comparison between numerical and experimental results of pressure was shown. Both results show the same increasing rate and maximum pressure, approximately. But, because we did not know chemical formula of diesel fuel in experiments, so delay time for combustion between CFD and experiment is not the same. Diesel fuel $C_{10}H_{22}$ was assumed for this simulation.

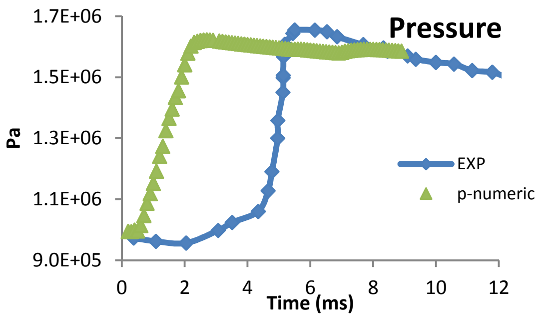

Figure 3. comparison CFD results with experimental data

RESULTS AND DISCAUTION

In Figs. 4(a, b, c), 5 (a, b, c) temperature field of fluid and solid phase of PM in middle angular cross section in three times, are shown. As seen in Figs. 4 (a,b), due to existence of solid phase of PM and exchange of heat with fluid phase, temperature decrement near injector location compensates. On the other hands, in locations where combustion occurs, temperature goes up considerably. Heat absorbs with solid phase and temperature of it increases. Figs. 5 (a,b) shows increase solid-temperature in locations where temperature goes up considerably. But heat capacity of solid is much higher than heat capacity of fluid; therefore increase in its temperature is much lower than fluid temperature. In Fig. 11c, it is seen that near the end of combustion, fluid temperature decreases and low value of NO relative to conventional combustion is form. In the region with high temperature, low oxygen exists, so possibility of NO formation decreases noticeable. Solid phase of PM acts like a controller for temperature.

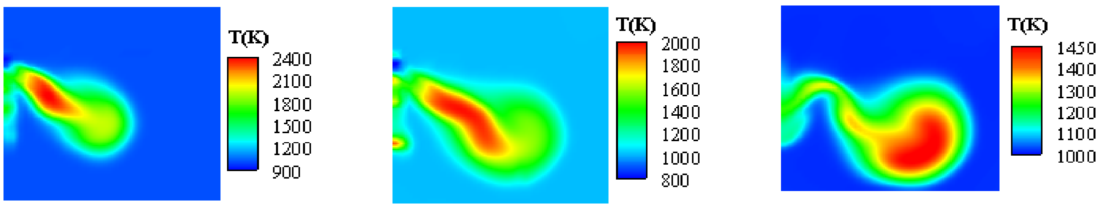

a) 1 ms b) 2 ms c) 3 ms

Fig 4. Fluid temperature in free volume

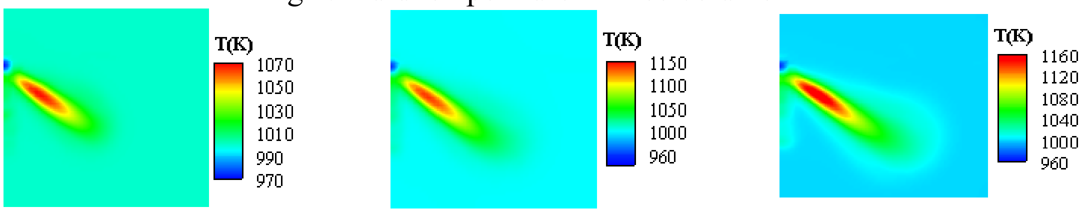

a)1 ms b) 2 ms c) 3 ms

Fig 5. Fluid temperature in PM reactor

Diesel spray in PM and effect of mass of injected fuel in constant porosity on combustion process

In Fig. 6, mass fraction of diesel vapor versus time (1 to 3ms) is shown. Initial conditions of 11 bar for pressure, 1000 K for both phase of PM, porosity of 90 percent with pore density of 8 ppi, were assumed. In these figures mass of injected fuel has changed between 10 to 30 mg (mixture between lean to rich). In this figure mass fraction of injected fuel changed. It is inferred that variation of fuel injection has effects on fuel distribution, but final mass fraction of fuel is about zero.

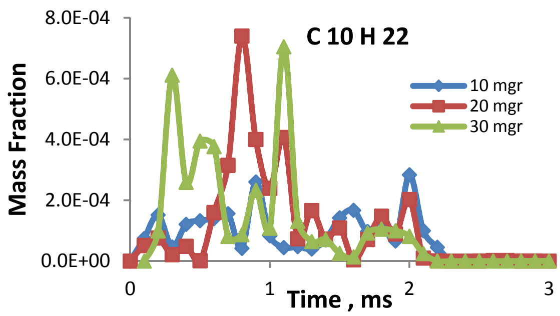

Figure 6. Mean diesel mass fraction versus time for porosity 90 % and different injected fuel

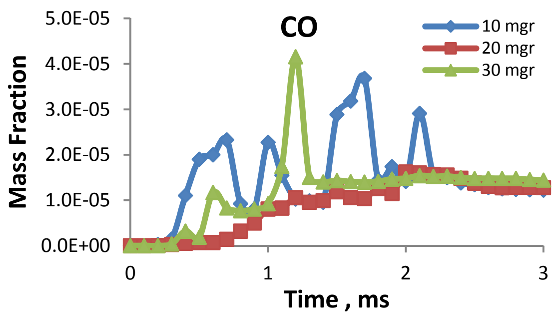

Figure 7. Mean Carbone monoxide mass fraction versus time for porosity 90 % and different injected fuel

Figs.7,8 show mass fraction of CO and NO versus time (1 to 3ms). Carbon monoxide is produced 0.5 ms after start of injection and increases gradually during of injection. But after end of injection, it does not change considerably. It is inferred that CO in PM engines has low value compared with conventional diesel engine. Because diesel disperses in PM volume and enough oxygen is accessible for combustion. Thereby, much of CO that is produced in combustion could convert to CO_2. Mean fluid temperature is below 1800 K (approximately bellow 1500 K), so thermal NO that produced during combustion has low value. Therefore, PM technology could control emission of CO and NO for different conditions. Fig. 9 represents mean pressure versus time (1 to 3ms). It is seen that with increasing mass of injected fuel, causes to increase final pressure as expected. Also, with increase injected fuel, rate of pressure also, increases.

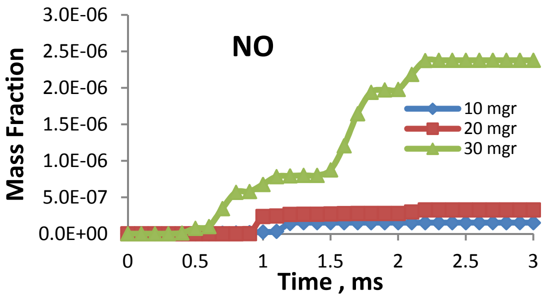

Figure 8. Mean nitrogen monoxide mass fraction versus time for porosity 90 % and different injected fuel

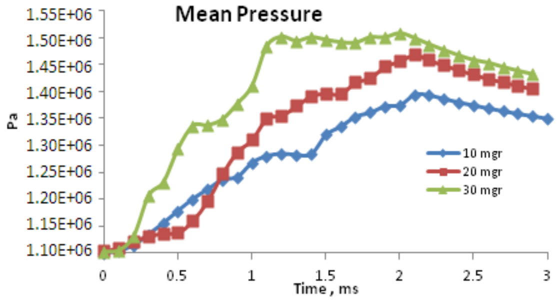

Figure 9. Mean pressure versus time for porosity 90 % and different injected fuel

Figs. 10, 11 shows mean temperature in fluid phase and solid phase of PM via time. It is seen that with increasing fuel lead to increase in fluid-phase temperature of PM. In solid-phase temperature, with increasing injected fuel, solid phase temperature does not varied. This phenomenon is due to heat capacity of PM is very higher than fluid phase. So, considerable change in fluid-phase temperature does not cause to considerable change in solid-phase temperature.

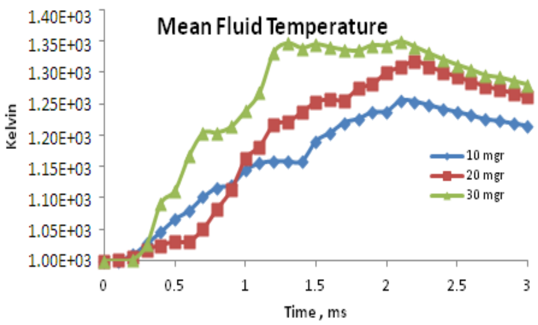

Figure 10. Mean fluid phase temperature versus time for porosity 90 % and different injected fuel

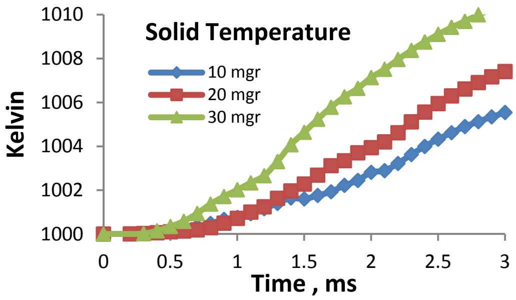

Figure 11. Mean solid phase temperature versus time for porosity 90 % and different injected fuel

CONCLUSIONS

3D- spray of diesel fuel in a hot PM was simulated with modified version of KIVA-3V code. The contours of mass fraction of diesel vapor, carbon dioxide, pressure and temperature in both phase of PM, were shown. Following results were obtained:

1) PM helps to better dispersion of fuel and flammable mixture formation in its space.

2) PM considerably contributes to the flame stabilization and nearly homogenizes temperature field.

3) Very thick reaction zone (hundred times thicker than for free flames in conventional combustion) formats in PM volume.

4) Pressure loss in PM due to its drag, is not significant in the case of the PM with high porosity.

5) Fuel vapor consumes completely, so nearly no HC residues in cylinder space.

6) Maximum value of fluid temperature decreases, therefore NO formation reduces due to lower temperature of fluid.

7) Increasing mass of injected fuel in hot PM increases pressure and fluid temperature but does not causes to CO, HC and soot formation.

NOMENCLATURE

c_p	specific heat of mixture
c_s	specific heat of solid medium
$D_{\parallel}^{d}$	thermal dispersion coefficient
h_i	enthalpy of species i
h_v	volumetric heat transfer coefficient of PM
k_g	thermal conductivity of the fluid
k_s	thermal conductivity of solid
q_r	radiation heat transfer in solid
T_g	gas temperature
T_s	solid temperature
$\bar{W}$	average molecular weight of mixture
X_i	molar fraction of species i
ρ_g	mixture density
ε	porosity of porous medium
$\acute{\omega}_i$	rate of reaction i
ρ_s	solid density

9. REFRENCES

[1] Weclas, M, Potential of porous medium combustion technology as applied to internal combustion engine, ISSN 1616-0762 Sonderdruck Schriftenreihe der Georg-Simon-Ohm-Fachooochule, Nurnberg, Germany, 2001
[2] Weclas, M., Strategy for intelligent internal combustion engine with homogeneous combustion in cylinder, Sonderdruck Schriftenreihe University of Applied Sciences in Nuernberg, NO. 26, pp. 1–14, 2004.
[3] Periasamy, C., Chinthamony, S. K., Gollahalli, S. R., Experimental evaluation of evaporation enhancement with porous media in liquid-fuel burners", J. Porous media, Vol. 10, Issue. 2, pp. 137-150, 2007.
[4] Kamal, M. M., Mohamad, A. A., Investigation of liquid fuel combustion in a cross flow burner. Proceedings of the Institution of Mechanical Engineers: Part A – Journal of Power and Energy, 221, pp. 371–385, 2007.

[5] Monmont, F. B. J., Van-Odyck, D. E. A., Nikiforakis, N. Experimental and theoretical of the combustion of n-tridecane in porous media, J. Fuel, Vol. 93, pp. 28-36, 2012.
[6]Wu, D., Liu, H., Xie, M., Liu, H., Sun, W., Experimental investigation on low velocity filtration combustion in porous packed bed using gaseous and liquid fuel, J. Experimental Thermal and Fluid Science, Vol. 36, pp. 169-177, 2012.
[7] Durst, F., Weclas, M., A new type of internal combustion engine based on the porous medium technology, J. Atomobile Engineering, IMechE, Part D, Vol. 215, pp. 63-81, 2001.
[8] Durst, F., Weclas, M., A new Concept of I.C engine with homogeneous combustion in a porous medium(PM), 5th International Symposium on Diagnostic and Modeling of Combustion in Internal Combustion Engines, COMODIA, Nagoya, Japan, 2001.
[9] Le, D. C., Chein, C. J., Kwak, Y. H., Improving surface characteristic of porous media reactor in diesel engine by plasma technology, F2006C27, 2006.
[10] Weclas, M., Ates, B., and Vlachovic, V., Basic aspects of interaction between a high velocity Diesel jet and highly porous medium (PM) 9th Int. Conference on Liquid Atomization and Spray Systems ICLASS, 2003.
[11] Weclas., M., High Velocity CR Diesel Jet impingement on to porous structure and its utilization for mixture homogenization in I.C. engines. DITICE Workshop: Drop/Wall interaction: industrial applications, Experiments and modeling, Bergamo, Italy, 2006.
[12] Weclas, M., Faltermeier, R., Diesel jet impingement on small cylindrical obstacles for mixture homogenization by late injection strategy, Int. J. Engine Research, Vol. 8, pp. 399-413, 2007.
[13] Weclas, M., Some fundamental observation on the diesel jet destruction and spatial distribution in highly porous structure, J. Porous Media, Vol. 11, Issue. 2, pp. 125-144, 2008.
[14] M. Weclas, porous media in internal combustion engine, M. Scheffle, P. Colombo, editors, Cellular ceramics-structure , manufacturing, properties and application, Wiley, 2005.
[15] Weclas., M., Cypris., J., Distributed-nozzle concept: a method for diesel spray distribution in space for charge homogenization by late injection strategy, 23rd Annual Conference on Liquid Atomization and spray systems, Brno, Czech Republic, 2010.
[16] Amsden., A. A., O'Rourke, P. J., and Butler, T. D., " KIVA-II: A Computer Program for Chemically Reactive Flows with Sprays", Los Alamos National Laboratory Report LA-11560-MS, Los Alamos, 1989.

[17] A. Mohammadi, A. Jazayeri, M. ziabasharhagh, Numerical simulation of direct injection engine with using porous medium, ICES 2012, Italy, 2012.
[18] P. K. Senecal, D. P. Schmidt, I. Nouar, C. J. Rutland, R. D. Reitz, M. L. Corradini, Modeling high-speed viscous liquid sheet atomization, Int. J. of Multiphase Flow, Vol. 25, pp. 1073-1097, 1999.